Radiotherapy and Oncology 162 (2021) 105–111

Contents lists available at ScienceDirect

Radiotherapy and Oncology

journal homepage: www.thegreenjournal.com

Original Article

Margin calculation for multiple lung metastases treated with single-isocenter SBRT

Janita E. van Timmeren [a,*], Mischa S. Hoogeman [b], Stefanie Ehrbar [a], Michael Mayinger [a], Nicolaus Andratschke [a], Matthias Guckenberger [a], Stephanie Tanadini-Lang [a]

[a] Department of Radiation Oncology, University Hospital Zürich and University of Zürich, Switzerland; [b] Erasmus MC Cancer Institute, University Medical Center Rotterdam, Department of Radiotherapy, The Netherlands

ARTICLE INFO

Article history:
Received 11 April 2021
Received in revised form 31 May 2021
Accepted 1 July 2021
Available online 10 July 2021

Keywords:
Stereotactic body radiotherapy
Lung cancer
Single isocenter multiple targets
Margin calculation

ABSTRACT

Background and purpose: A single-isocenter stereotactic body radiotherapy (SBRT) approach for multiple lung metastases has the potential to lower cumulative patient dose and reduce overall treatment time. However, the magnitude of inter-lesion position variation is currently unknown and not incorporated in margin calculations. The aim of this study was to quantify inter-lesion position variation and calculate safety margins for single-isocenter lung SBRT.

Materials and methods: A total of 83 pairs of pulmonary metastases from 42 NSCLC patients were used to calculate relative inter-lesion position variation by lesion-based registration of planning CT and verification CBCT. Furthermore, β-value assessment of van Herk's margin formula was performed by evaluating the distance between planned and blurred dose profiles of simulated spherical lesions, to evaluate its validity for heterogeneously planned dose distributions. Population-based ITV to PTV margins were calculated using the entire dataset and using subgroups with significant differences in relative inter-lesion position variation.

Results: The mean ± SD inter-lesion position variation was 1.2 ± 1.1 mm as 3D-vector. Inter-lesion position variation was significantly increased if ≥1 lesion was not attached to the pleura or lesions were distant. The simulation showed that the combined SD of the random errors contributed to the margin only in the SI direction with $0.25 \cdot \sigma_{tot}$ for a 65% dose prescription. When incorporating inter-lesion position variation, the safety margins increased from 5.6, 5.8, 5.2 mm (AP, SI, LR) to 6.0, 6.6, 5.5 mm for the entire cohort.

Conclusion: Relative inter-lesion position variation is influenced by inter-target distance and location and can be compensated with additional safety margins of <1 mm using single-isocenter SBRT.

Stereotactic body radiotherapy (SBRT) is increasingly used for oligometastatic disease, including non-small cell lung cancer (NSCLC) [1–4]. The current standard solution for patients presenting with more than one lesion is to use multiple isocenters, i.e. one for each lesion. This requires cone-beam CT (CBCT) guided treatment positioning verification multiple times during treatment. This results in prolonged overall treatment times, and intra-treatment patient motion could cause unforeseen overlap of dose distributions in an organ-at-risk (OAR). Furthermore, long treatments are challenging for patients, especially for patients with pain and the elderly.

Using a single isocenter for multiple targets in combination with intensity-modulated radiotherapy (IMRT), or volumetric modulated arc therapy (VMAT), recently gained interest. It may result in a more efficient workflow, reduce the number of monitor units (MU) and thereby reduce the cumulative patient dose, overall planning/treatment time, and improve cost-effectiveness [5–10]. However, a major challenge in lung SBRT as opposed to intracranial single-isocenter treatments, is that different parts of the lung are known to move independently, and the inter-target distance may vary on a day-to-day basis [11]. Therefore, the possibility that multiple targets move and rotate relative to each other has to be taken into account for internal target volume (ITV) to planning target volume (PTV) margin definition.

In this study we quantified the relative inter-lesion position variation based on data from patients treated for two or more lung metastases and additionally assessed the β-value of van Herk's margin formula through the simulation of planned and blurred

* Corresponding author at: Department of Radiation Oncology, University Hospital Zürich and University of Zürich, Rämistrasse 100, 8091 Zürich, Switzerland.
E-mail address: janita.vantimmeren@usz.ch (J.E. van Timmeren).

https://doi.org/10.1016/j.radonc.2021.07.001
0167-8140/

dose profiles, with the final aim to calculate safety margins for a single-isocenter technique.

Materials and methods

Patients

Between 2018 and 2019, a total of 42 patients with 44 SBRT courses were identified for this retrospective study. Patients were treated for > 1 intrapulmonary lesion: patients were treated for two (n = 26), three (n = 15), four (n = 1), six (n = 1) or seven (n = 1) pulmonary metastases using a conventional linear accelerator (linac) (Varian Truebeam model). Patients were immobilized in a vacuum cushion. A six degrees-of-freedom couch was available and during set-up the patient position was corrected in all six dimensions. Typically, patients received one CBCT scan per treatment plan prior to each fraction (Table 1). During irradiation patient position was monitored using the RPM patient positioning monitoring (Varian Medical Systems, Palo Alto, CA). Ethics approval of this study was received by the local ethics commission (BASED-Nr.2018-01750). All patients gave informed consent for use of their data.

For all patients a planning CT (pCT) acquired with a Siemens SOMATOM Definition AS Open (Siemens AG, Germany) and at least one CBCT, with a field of view (FOV) covering at least two lesions, were available. All possible combinations of two individual lesions were included in the calculation of the systematic and random errors caused by relative inter-lesion position variation. Lesions were not considered in case they were not in the FOV (n = 9) or not visible on the CBCT (n = 2). This resulted in 83 lesion-pairs. Characteristics of all pulmonary metastases are presented in Table 1.

Table 1
Characteristics of the 42 patients with multiple metastases included for the calculation of relative inter-lesion position variation.

Number of patients		**42**
Number of treatments		**44**
Number of lesions per treatment		2 (n = 26) 3 (n = 15) 4 (n = 1) 6 (n = 1) 7 (n = 1)
Lesion volume [cm^3]		
Median [range]		1.8 [0.1–38.3]
Mean ± SD		4.6 ± 6.8
Number of treatment plans*		**86**
Number of fractions per treatment plan		3 (n = 5) 5 (n = 58) 7 (n = 1) 8 (n = 14) 10 (n = 8)
Number of lesion-pairs		**83****
Inter-target distance [cm]		
Median [range]		7.2 [1.0–24.3]
Mean ± SD		8.6 ± 5.6
At least one lesion not attached to the pleura		yes (n = 65) no (n = 18)
Both lesions not attached to the pleura		yes (n = 37) no (n = 46)
Lesions in the same lung		yes (n = 60) no (n = 23)
Lesions in the same lobe		yes (n = 42) no (n = 41)
At least one lesion in the lower lobe		yes (n = 49) no (n = 34)
Number of lesions		**104**
Lesion location†		
Right lung		n = 62
	Lower lobe	n = 19
	Middle lobe	n = 7
	Upper lobe	n = 31
Left lung		n = 42
	Lower lobe	n = 19
	Upper lobe	n = 20
Attached to the pleura		yes (n = 43) no (n = 61)

*For 14 patients, either both lesions or two out of three lesions were grouped and treated with a single isocenter in the original clinical treatment plans.
**All possible lesion-pairs were included in the error calculation.
†*Six lesions were location centrally/in the lymph nodes.*

Relative motion error

To assess relative inter-lesion position variations, manual lesion-based registrations of the average 3D pCT (1.0 × 1.0 × 2.0 mm^3) and the verification CBCT (0.9 × 0.9 × 2.0 mm^3) were performed in the Offline Review application of Eclipse treatment planning system (TPS) (Varian Medical Systems, Palo Alto, CA). The required shifts in anterior-posterior (AP), superior-inferior (SI) and left–right (LR) direction to obtain the visually best possible registration between the lesions on the CBCT and pCT images, were noted.

For the assessment of the relative position variation error we evaluated two possible image-guided radiotherapy (IGRT) motion compensation strategies in the single-isocenter situation. The first IGRT strategy was to correct such that the average shift between both lesions is compensated. Then, the same margin needs to be applied for all lesions. The second IGRT strategy aimed at optimal alignment of largest lesion or the lesion closest to a critical OAR. Because of independent lesion movement, the remaining lesion (s) are at higher risk of position errors, which needs to be compensated with adapted margins for each lesion. The two IGRT approaches are illustrated in Figs. A.1 and A.2, the latter showing a real registration example.

The margin calculation itself is the same for both IGRT approaches, but both approaches require a different assessment of the relative position variation errors, and thus subsequent margins will be different.

Approach 1

For approach 1, the shifts per lesion were averaged to obtain the shift per fraction. Next, we calculated an average and standard deviation (SD) per lesion-pair. These were then used to estimate the SD of the systematic relative position variation error (Σ_{rpv}) and the SD of the random relative position variation error (σ_{rpv}), by taking the SD (of the per lesion-pair averages) and root mean square (RMS) (of the per lesion-pair SDs), respectively. This was repeated for all three directions (AP, LR and SI). The assessment of Σ_{rpv} and σ_{rpv} is illustrated in Fig. A.3.

Approach 2

For approach 2, the shifts per lesion were not averaged, but the difference was calculated (representing the situation that the alignment is optimal for only one lesion, see also Figs. A.1 and A.2). These differences were then used to calculate the average and SD per lesion-pair. Subsequently, these were used to estimate Σ_{rpv} and σ_{rpv}, by calculating the SD and RMS, respectively. This was repeated for all three directions (AP, LR and SI).

The magnitude of the systematic and random errors due to relative position variation was assumed to be dependent on distance between the lesions, location of the lesions (e.g. in which lobe, or both in the same lung or lobe) and the presence of possible movement restrictions (e.g. attached to the pleura). Therefore, the average shifts in AP, LR and SI and the 3D vector were evaluated for these different situations in order to investigate whether different margins were desirable. Wilcoxon rank-sum test in R (version 4.0.2) was used to evaluate differences. P-values below 0.05 were considered significant. The inter-target distances were calculated

using the x-, y- and z-primary coordinates of the tumor centers in the TPS. Population-based margins were calculated for different subgroups depending on significant differences between the inter-lesion shifts.

Margin calculation

The van Herk formula was used to calculate the ITV (defined as the union of the gross tumor volumes on the 4DCT) to PTV margin (formula 1) [12,13].

$$M = M_r + M_s = \beta\sqrt{\sigma_{tot}^2 + \sigma_p^2} - \beta\sigma_p + \alpha\Sigma_{tot} \approx \beta_{heterogeneous}\sigma_{tot} + \alpha\Sigma_{tot} \quad (1)$$

Systematic and random errors

The combined SD of all random errors were calculated as $\sigma_{tot} = \sqrt{\sigma_{rpv}^2 + \sigma_{im}^2 + \sigma_{linac}^2}$ for the margin contribution of the random errors M_r, and the combined SD of all systematic errors as $\Sigma_{tot} = \sqrt{\Sigma_{rpv}^2 + \Sigma_{im}^2 + \Sigma_{del}^2}$ for the margin contribution of the systematic errors M_s. The SD of the systematic error in the delineation (Σ_{del}) was assumed to be 2 mm, as described before for small lesions [14]. The SD for systematic and random errors caused by intra-fractional baseline shift (Σ_{im} and σ_{im}), i.e. tumor displacement in pre- and post-treatment CBCT, were calculated before [15]. The SD of the random error due to mechanical inaccuracy of the linear accelerator (σ_{linac}) was assumed to be 0.6 mm based on the 90th percentile of the maximum measured radius during routinely performed Winston-Lutz tests (Table 2).

Moreover, since multiple lesions move independently, additional relative position variation errors (Σ_{rpv} and σ_{rpv}) were introduced in the margin calculation to account for the errors in the positioning verification process. The margins with and without relative position variation error were assessed and compared.

Beta value

Beta is a dimensionless constant, which when multiplied by the combined SD of the random errors, represents the distance between the 50% and X% isodose surfaces of the blurred dose distribution, with X being the prescription level [12]. The lower the prescription isodose surface, the lower beta is.

Since van Herk's formula was derived for homogenous dose distributions which are not used in SBRT, we performed a dosimetric evaluation of the penumbra in order to assess the contribution of random errors M_r ($\approx \beta_{heterogeneous}\sigma_{tot}$). To this extent, for two patients a spherically shaped tumor with a 3 cm or 2.5 cm diameter was simulated in both lung and liver (the latter for potential future applications). To simulate tumor tissue, the density of the spheres in the lung were overridden with the mean density of the existing tumors. Dose normalization was done such that the prescription isodose line corresponds to either 65% or 80% of the maximum dose. The Acuros XB (version 15.6.03) dose calculation algorithm was used. After treatment planning, dose profiles were extracted in AP, SI and LR direction (Fig. B.1). The profiles were imported in Matlab 2019a (MathWorks Inc, Natick, MA) and convoluted with a Gaussian filter with σ-values ranging from 1 to 10 mm using the function *smoothdata*. The distance between the planned profile and the blurred profile was calculated for the 100% isodose line covering the PTV for each σ. These distances were plotted against the σ-values, followed by a linear regression; the slope then corresponded to $\beta_{heterogeneous}$. Since $\beta_{heterogeneous}$ was assessed through blurring dose profiles, the correction for the SD of the penumbra width (σ_p) is included automatically.

This approach of assessing $M_r$was then compared to the conventional $\beta\sqrt{\sigma_{tot}^2 + \sigma_p^2} - \beta\sigma_p$. Here, a β-value of 0.39 was used, which corresponds to a prescription level of 65%, which was found by taking the inverse of the standard normal cumulative distribution with a probability of 0.65 [12]. It was assessed at which σ_p the two approaches were in agreement.

Alpha value

Alpha is a dimensionless constant that multiplied with the systematic error yields the margin for systematic errors at a given confidence level. In formula 1, α equals 2.5 was used which represents the situation where systematic errors in all three directions have an influence and assumes that 90% of the population receives a cumulative ITV dose of at least 95%.

Fractionation

The median number of fractions was 4.5 for Σ_{im} and σ_{im} [15]. In the current study, Σ_{rpv} and σ_{rpv} were determined using mainly 5-fraction treatments (Table 1). Therefore, the margin calculation presented here is applicable for 5 fractions. The margins for 3, 8 and 10 fraction-treatments are presented in Supplementary Material C.

Results

The locations of all lesion pairs are schematically presented in Fig. 1. The median [inter-quartile range] absolute average shift considering all lesion pairs was 0.6 mm [0.3 mm–1.1 mm] in SI, 0.3 mm [0.1 mm–0.5 mm] in LR and 0.4 mm [0.1 mm–0.7 mm] in AP. The median [range] of the 3D vector of the average inter-lesion position variation was 1.1 mm [0.6 mm–1.5 mm].

The median inter-target distance was 7.2 cm. The inter-lesion position variation as a 3D vector was significantly larger if at least one lesion was not attached to the pleura (p = 0.015) or when both lesions were not attached (p = 0.043) (Fig. A.4). Additionally, the average inter-lesion position variation for distant lesions (≥median of 7.2 cm) was significantly different for AP (p = 0.016) and LR (p = 0.0016) compared to proximal lesions (<7.2 cm). When both lesions were in the same lobe the inter-lesion position variations were significantly larger in LR (p = 0.0011). There were five outliers with largest relative inter-lesion motion (Figs. 1 and 2). These lesion-pairs had in common that at least one lesion was not

Table 2
Standard deviations of the systematic and random errors to be considered for margin calculation. Delineation error and errors due to inter-fractional baseline shift were retrieved from literature [14,15]. Errors due to linac mechanical accuracy were defined as the 90th percentile of the maximum radius measured during routinely performed Winston-Lutz tests.

	Systematic errors Σ [mm]			Random errors σ [mm]		
	AP	SI	LR	AP	SI	LR
Delineation	2	2	2	–	–	–
Intra-fractional shift	1.0	1.0	0.5	1.1	0.7	0.8
Linac	–	–	–	0.6	0.6	0.6

*AP = anterior-posterior, SI = superior-inferior, LR = left–right.

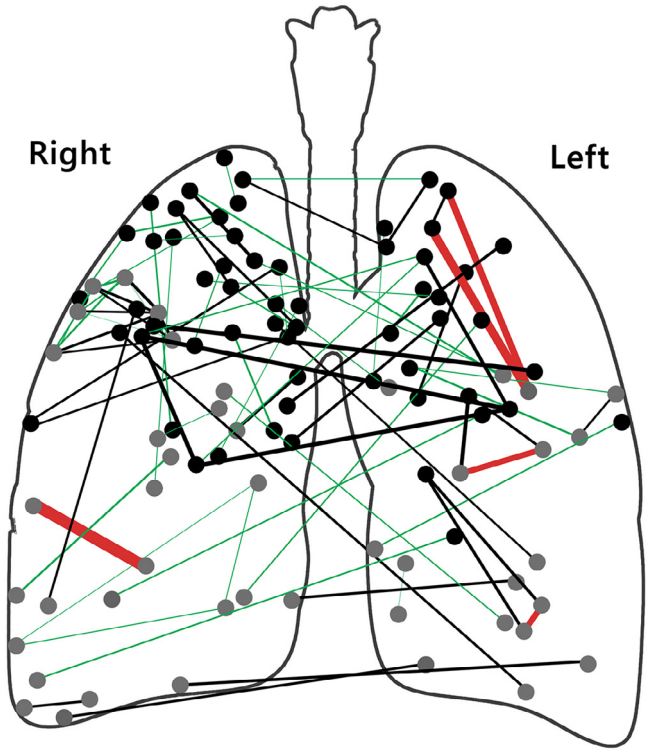

Fig. 1. Lesions' location in the lungs. All lesion-pairs that were used for relative inter-lesion position variation assessment, schematically projected in the lungs. Lesions located in the middle (right lung) or lower lobe are colored in grey. Line thickness is proportional to the magnitude of the 3D motion vector. Green lines indicate a shift smaller than the median (<1.1 mm) and black lines indicate a shift larger than the median (>1.1 mm). Red lines indicate the five outliers with large inter-lesion position variation.

attached to the pleura and at least one lesion was present in a lower lobe.

The population-based systematic and random errors due to relative inter-lesion position variation are shown in Table A.1.

These results indicate that pleural attachment and inter-target distance significantly influence relative inter-lesion position variation. We assumed distance to be a surrogate for whether the lesions are in the same lobe or not, i.e., lesions in the same lobe have short inter-lesion distance. To this extent, population-based margins were calculated for the entire cohort, as well as for the following three groups: (1) patients with at least one lesion without pleural attachment and large inter-lesion distance (≥7.2 cm), (2) as (1), but small inter-lesion distance and (3) patients with pleural attachment of all lesions. The 3D vectors of the average shifts are shown in Fig. 2, and the systematic and random relative position variation errors for the entire cohort and for these three groups is shown in Table 3.

The simulation of spherical lesions showed that for a 65% dose prescription, the 100% isodose line coincides with the symmetric point in the AP and LR dose profiles and is thus invariant to blurring (Fig. 3). For SI, a σ_p of 5.2 mm resulted in the best visual correspondence between simulation and calculation (Fig. B.2-A). The final value of $\beta_{heterogeneous}$ through simulation was 0.25 (Table B.1). For the 80% dose prescription, the results are also shown in Fig. 3, Fig. B.2-B and Table B.1.

Using these calculated values for the simulated $\beta_{\text{heterogeneous}}$-value of 0.25, the relative inter-lesion position variation errors, the errors of Tables 2 and 3, and formula 1, the ITV to PTV margin was calculated for all groups, for approach 1 and 2, and for multiple-isocenter treatments (Table 3). The maximum difference between groups was 0.8 mm for approach 1, and 1.9 mm for approach 2.

The largest observed difference between the 3-fraction and 10-fraction margin for the 65% isodose prescription was 0.5 mm for approach 2 in group 1 for the AP and SI direction (Tables C.1 and C.2).

Discussion

Single-isocenter lung SBRT is an emerging technique for oligometastatic disease [5–9]. Nevertheless, there are little data about treatment margins for this technique taking into account relative inter-lesion position variation. Therefore, this study aimed to

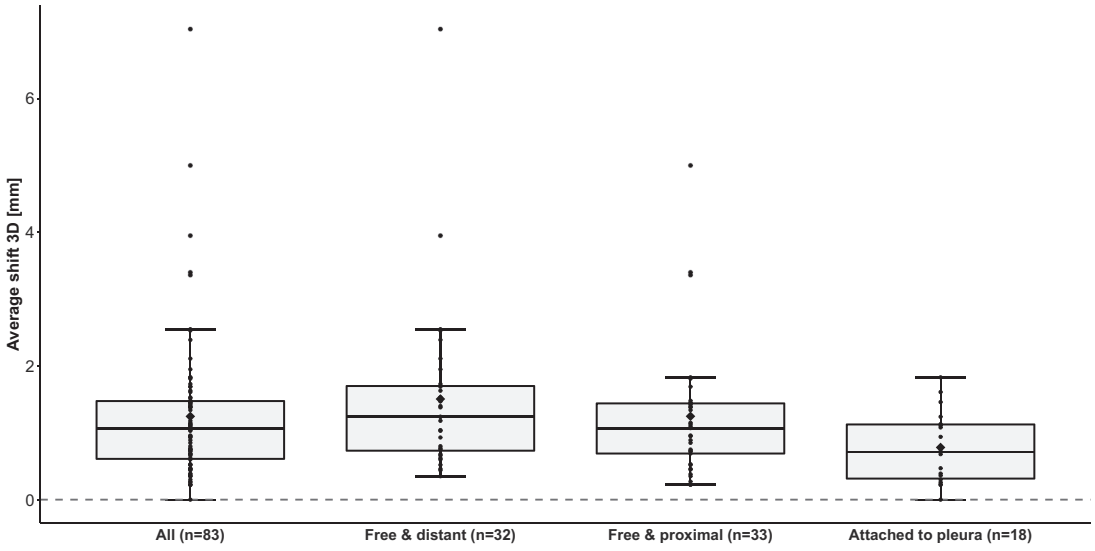

Fig. 2. Average shift in 3D. Average CT to CBCT shift in 3D, for all lesion-pairs (left), lesion-pairs for which at least one lesion without pleural attachment ('free') and the lesions were distant (second), patients for which at least one lesion without pleural attachment ('free') and the lesions were proximal (third) and patients for which all lesions were attached to the pleura (right). The green diamonds represent the mean.

Table 3
Systematic and random relative motion errors as well as calculated margins for a treatment with 5 fractions and a 65% isodose prescription. Approach 1: CT/CBCT registration that results in an average match for all lesions. Approach 2: CT/CBCT registration that results in the best possible match for the largest lesion. Group 1: patients that have at least one lesion without pleural attachment and have the lesions distant (>median). Group 2: patients that have at least one lesion without pleural attachment and have the lesions proximal (<median). Group 3: patients that have both lesions attached to the pleura.

		Systematic errors Σ_{rpv} [mm]			Random errors σ_{rpv} [mm]			Margin [mm]		
		AP	SI	LR	AP	SI	LR	AP	SI	LR
Approach 1	All (n = 83)	0.9	1.1	0.8	0.8	1.0	0.7	6.0	6.6	5.5
	Group 1 (n = 32)	1.2	1.2	1.0	1.0	1.3	0.8	6.4	6.7	5.8
	Group 2 (n = 33)	0.7	1.3	0.6	0.6	0.8	0.8	5.9	6.8	5.4
	Group 3 (n = 18)	0.5	0.6	0.6	0.5	0.6	0.4	5.7	6.0	5.4
Approach 2	All (n = 83)	1.6	1.6	1.4	1.2	1.5	1.1	6.9	7.3	6.2
	Group 1 (n = 32)	2.3	2.1	1.9	1.6	2.1	1.4	8.0	8.2	7.0
	Group 2 (n = 33)	1.0	1.4	0.8	0.9	1.0	0.9	6.1	7.0	5.5
	Group 3 (n = 18)	1.0	1.0	1.0	0.7	1.0	0.8	6.1	6.4	5.8
	No relative motion error	0	0	0	0	0	0	5.6	5.8	5.2
Multiple isocenters treatment		0	0	0	0	0	0	5.6	5.8	5.2

*AP = anterior-posterior, SI = superior-inferior, LR = left–right.

calculate safety margins accounting for relative inter-lesion shifts using a single-isocenter SBRT technique.

Relative inter-lesion position variation was shown to be dependent on inter-target distance and intrapulmonary lesion location. Surprisingly, when lesions were located in both lungs, this did not result in significantly increased relative position variation. This may result from the synchronized movement of both lungs according to the contraction of the diaphragm. Generally, the resulting margins are only marginally different between the groups, especially for approach 1 with a maximum difference of 0.8 mm. Larger differences were observed for approach 2 (maximum 1.9 mm), but since a smaller margin could be applied to lesions close to an OAR, this approach could still be beneficial.

Attention should be paid for individual cases that are at risk of large inter-lesion shifts (>3 mm as a 3D vector). The five patients in our study that were considered outliers (Fig. 1) all had at least one lesion in the lower lobe and at least one lesion not attached to the pleura. Therefore, for these cases careful comparison of the lesion positions between planning CT imaging and diagnostic CT imaging is recommended before deciding for a single-isocenter treatment. In the worst-case scenario re-planning into multiple-isocenter treatment plans is required in about 5% (5 outliers out of 83 lesion-pairs) of the cases.

The van Herk formula was used for margin calculations in this study. However, the van Herk formula is derived assuming homogeneous dose distributions with a perfect Gaussian penumbra. To the best of our knowledge, no study has investigated the β-value for heterogeneously planned lung SBRT. One study has performed experimental validation of the van Herk formula for lung radiotherapy, but also here a homogeneous dose distribution was assumed [16]. Our study shows that in case the SD of the width of the penumbra is 5.2 mm, the simulated value of $\beta_{heterogeneous}$ of 0.25 for the SI direction is in agreement with the theoretical β of 0.39 for a 65% prescription level. This result confirms that the simulation is a plausible approach for the assessment of the margin contribution by random errors.

In general, compared to the margins for multiple-isocenter treatments, the margins increased only slightly when incorporating relative inter-lesion position variation for single-isocenter treatments. Also, different fractionations resulted only in minor changes in the final margins (max 0.5 mm).

In the current study, the ITV concept was used to account for breathing motion. Therefore, the final margins can be transferred to a limited extend to other motion management techniques such as mid ventilation (mid-V) concept, gating or tracking [17]. For the mid-V concept, the inter-lesion motion should be assessed by matching the mid-V phase of the 4D-CT to the mid-V phase of the 4D-CBCT and for gating the inhale or exhale phase should be matched. However, we expect that these distances will be very similar and therefore our results on the inter-lesion motion could also be used for mid-V or gating margin calculations. For gating it additionally needs to be checked that the lesions are in the gating phase at the same time. For tracking, one would ideally track both tumors and adapt to their position using for example MLC tracking. A simpler approach would be to track one lesion and assume that the other lesion is moving in the same correlation to the first lesion as during planning CT, which is possible with CyberKnife using implanted fiducial markers. Nevertheless, this is not so straightforward in case of non-synchronous movements, thus more research is needed.

This study has a few limitations. The number of lesion-pairs in each group to calculate the errors due to position variation were relatively small. Larger numbers would result in a more precise estimation of population-based margins, and margin groups could be investigated better.

Only lesion-pairs located within the FOV of the CBCT were included in this study. Therefore, the longitudinal distance between lesions was always less than 7.5 cm, while the maximum inter-lesion distance in this study was as large as 24.3 cm.

Furthermore, the lesion-based registrations between pCT and CBCT were performed manually, which results in some uncertainty in the assessment of the inter-lesion position variation. A recent study showed that the mean differences between observers was less than 1 mm in all directions [18]. For testing purposes, we included a 'worst-case scenario' 1.0 mm random error in all three directions in the margin calculation, which resulted in a maximum difference of 0.2 mm in the margin, which was observed only for SI for 3-fraction treatments. For all other fractionation schemes or directions, the impact on the margin was at most 0.1 mm.

Moreover, the $\beta_{heterogeneous}$ value was estimated using only two patients with sphere-shaped lesions. A simulation with multiple lesions resulted in comparable $\beta_{heterogeneous}$ values (not shown),

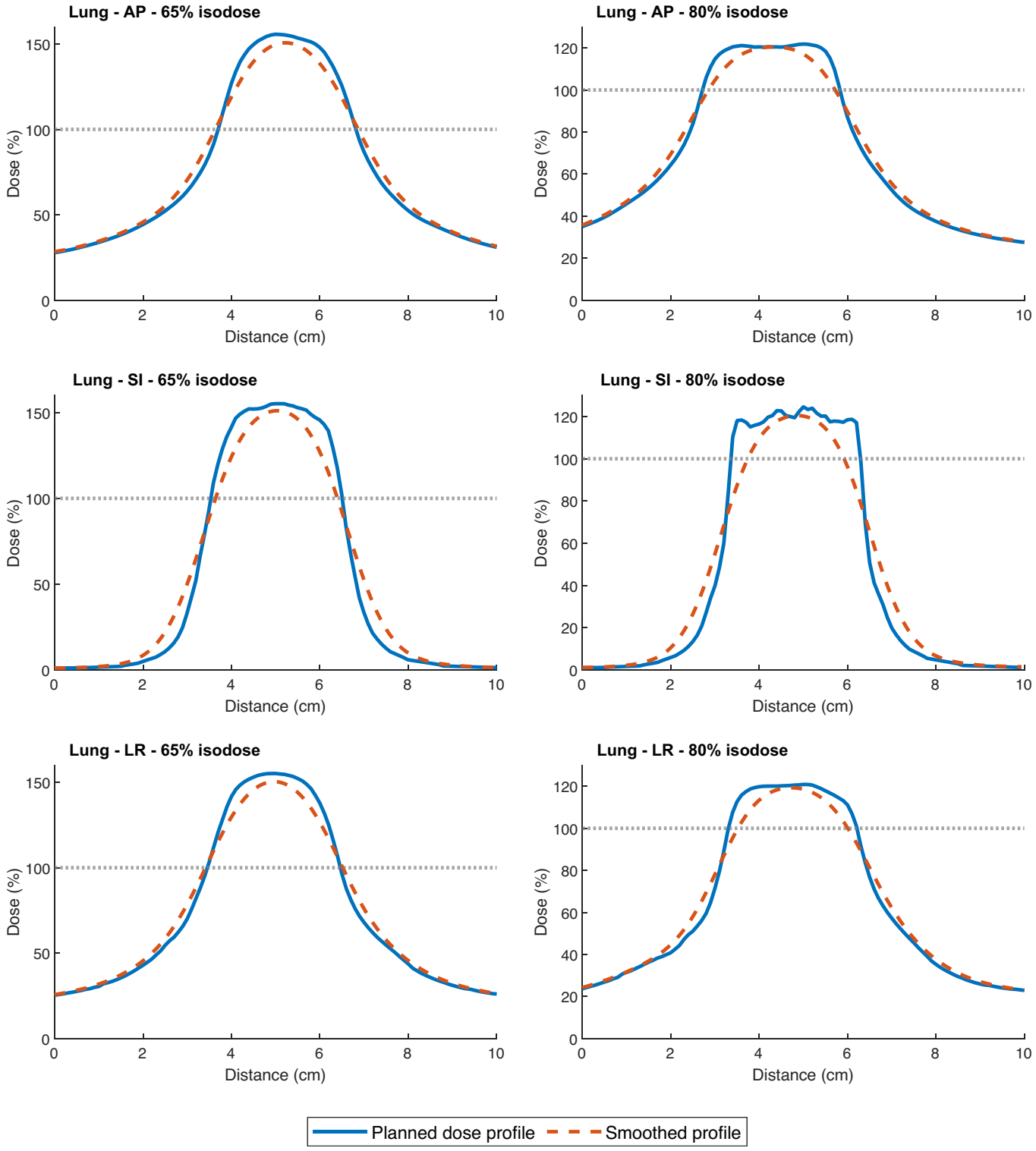

Fig. 3. Dose profiles. Dose profiles (blue lines) of a patient with an artificial lesion (3 cm diameter sphere) in the lung, optimized with a 65% isodose prescription (left column) or an 80% isodose prescription (right column). Orange dashed lines represent the blurred profiles using a Gaussian filter with a sigma of 6 mm. The horizontal dashed line at the 100% isodose line corresponds to the boundary of the tumor and is the location at which the distance between the 'planned' and 'blurred' dose distributions was measured to find $\beta_{\text{heterogeneous}}$.

but irregular shaped tumors were not investigated. But, since the contribution of the random errors to the final margins is small, this is not expected to have a large impact.

The margin calculation in our study did also not take into account that the dose conformity is generally not perfect, meaning that the 65% isodose line lies already outside the PTV in a realistic scenario.

In a recent report, the authors suggest to use a different α-value in the situation of multiple lesions [19]. The authors suggest to correct the confidence level according to the number of targets to

keep the combined uncertainty at 90% [20], which was not investigated in the current study.

The evaluation of the dosimetric impact of the single-isocenter approaches described in this study, was not within the scope of the current research, but will be performed in a future study.

Conclusions

Lesion individual margins were derived for single-isocenter lung SBRT, and relative inter-lesion position variation has only a small influence on the safety margin (maximum 1 mm). A subgroup of patients with at least one lesion without pleural attachment and at least one lesion located in the lower lobe was characterized by increased relative inter-lesion position variation and single-isocenter SBRT should be evaluated more carefully.

Conflict of interest statement

Dr. Hoogeman reports grants from Elekta, grants from Accuracy, grants from Varian, other from Accuracy, outside the submitted work. Dr. Tanadini-Lang reports that her husband works at Varian Medical Systems. Dr. van Timmeren, dr. Ehrbar, dr. Mayinger, dr. Andratschke and dr. Guckenberger report no conflict of interest.

Appendix A. Supplementary data

Supplementary data to this article can be found online at https://doi.org/10.1016/j.radonc.2021.07.001.

References

[1] Guckenberger M, Lievens Y, Bouma AB, Collette L, Dekker A, deSouza NM, et al. Characterisation and classification of oligometastatic disease: a European Society for Radiotherapy and Oncology and European Organisation for Research and Treatment of Cancer consensus recommendation. Lancet Oncol 2020;21:e18–28. https://doi.org/10.1016/S1470-2045(19)30718-1.

[2] Palma DA, Olson R, Harrow S, Gaede S, Louie AV, Haasbeek C, et al. Stereotactic ablative radiotherapy for the comprehensive treatment of oligometastatic cancers: long-term results of the SABR-COMET Phase II randomized trial. J Clin Oncol 2020;38:2830–8. https://doi.org/10.1200/JCO.20.00818.

[3] Iyengar P, Wardak Z, Gerber DE, Tumati V, Ahn C, Hughes RS, et al. Consolidative radiotherapy for limited metastatic non-small-cell lung cancer: a phase 2 randomized clinical trial. JAMA Oncol 2018;4:e173501. https://doi.org/10.1001/jamaoncol.2017.3501.

[4] Gomez DR, Tang C, Zhang J, Blumenschein GR, Hernandez M, Lee JJ, et al. Local consolidative therapy vs. maintenance therapy or observation for patients with oligometastatic non-small-cell lung cancer: long-term results of a multi-institutional, phase II, randomized study. J Clin Oncol 2019;37:1558–65. https://doi.org/10.1200/JCO.19.00201.

[5] Sanford L, Molloy J, Kumar S, Randall M, McGarry R, Pokhrel D. Evaluation of plan quality and treatment efficiency for single-isocenter/two-lesion lung stereotactic body radiation therapy. J Appl Clin Med Phys 2019;20:118–27. https://doi.org/10.1002/acm2.2019.20.issue-110.1002/acm2.12500.

[6] Trager M, Salama J, Yin FF, Adamson J. SBRT treatment of multiple extracranial oligometastases using a single isocenter with distinct optimizations. J Radiosurg SBRT 2017;4:265–73.

[7] Pokhrel D, Sanford L, Halfman M, Molloy J. Potential reduction of lung dose via VMAT with jaw tracking in the treatment of single-isocenter/two-lesion lung SBRT. J Appl Clin Med Phys 2019;20:55–63. https://doi.org/10.1002/acm2.12580.

[8] Sanford L, Pokhrel D. Improving treatment efficiency via photon optimizer (PO) MLC algorithm for synchronous single-isocenter/multiple-lesions VMAT lung SBRT. J Appl Clin Med Phys 2019;20:201–7. https://doi.org/10.1002/acm2.v20.1010.1002/acm2.12721.

[9] Quan K, Xu KM, Lalonde R, Horne ZD, Bernard ME, McCoy C, et al. Treatment plan technique and quality for single-isocenter stereotactic ablative radiotherapy of multiple lung lesions with volumetric-modulated arc therapy or intensity-modulated radiosurgery. Front Oncol 2015;5. https://doi.org/10.3389/fonc.2015.00213.

[10] Pokhrel D, Sanford L, Larkin S, Dhanireddy B, Bernard ME, Randall M, et al. On the use of single-isocenter VMAT plans for SBRT treatment of synchronous multiple lung lesions: plan quality, treatment efficiency, and early clinical outcomes. J Appl Clin Med Phys 2020;21:160–7. https://doi.org/10.1002/acm2.v21.810.1002/acm2.12938.

[11] Sarudis S, Karlsson Hauer A, Nyman J, Bäck A. Systematic evaluation of lung tumor motion using four-dimensional computed tomography. Acta Oncol 2017;56:525–30. https://doi.org/10.1080/0284186X.2016.1274049.

[12] van Herk M, Remeijer P, Rasch C, Lebesque JV. The probability of correct target dosage: dose-population histograms for deriving treatment margins in radiotherapy. Int J Radiat Oncol Biol Phys 2000;47:1121–35. https://doi.org/10.1016/S0360-3016(00)00518-6.

[13] VANHERK M. Errors and margins in radiotherapy. Semin Radiat Oncol 2004;14:52–64. https://doi.org/10.1053/j.semradonc.2003.10.003.

[14] Sonke J-J, Rossi M, Wolthaus J, van Herk M, Damen E, Belderbos J. Frameless stereotactic body radiotherapy for lung cancer using four-dimensional cone beam CT guidance. Int J Radiat Oncol Biol Phys 2009;74:567–74. https://doi.org/10.1016/j.ijrobp.2008.08.004.

[15] Lang S, Shrestha B, Graydon S, Cavelaars F, Linsenmeier C, Hrbacek J, et al. Clinical application of flattening filter free beams for extracranial stereotactic radiotherapy. Radiother Oncol 2013;106:255–9. https://doi.org/10.1016/j.radonc.2012.12.012.

[16] Ecclestone G, Bissonnette J-P, Heath E. Experimental validation of the van Herk margin formula for lung radiation therapy. Med Phys 2013;40:111721. https://doi.org/10.1118/1.4824927.

[17] Thomas SJ, Evans BJ, Harihar L, Chantler HJ, Martin AGR, Harden SV. An evaluation of the mid-ventilation method for the planning of stereotactic lung plans. Radiother Oncol 2019;137:110–6. https://doi.org/10.1016/j.radonc.2019.04.031.

[18] Kim B, Kirkby C, Semaka A, Debenham B, Campbell T. Assessment of IGRT variability for lung SBRT. J Med Imaging Radiat Sci 2021;52:191–7. https://doi.org/10.1016/j.jmir.2021.02.004.

[19] Tudor GSJ, Bernstein D, Riley S, Rimmer Y, Thomas SJ, van Herk M, et al. Geometric uncertainties in daily online IGRT: refining the CTV-PTV margin for contemporary photon radiotherapy. Br Inst Radiol 2020.

[20] Kershaw L, van Zadelhoff L, Heemsbergen W, Pos F, van Herk M. Image guided radiation therapy strategies for pelvic lymph node irradiation in high-risk prostate cancer: motion and margins. Int J Radiat Oncol Biol Phys 2018;100:68–77. https://doi.org/10.1016/j.ijrobp.2017.08.044.